ASME Journal of Energy Resources Technology
Online journal at:
https://asmedigitalcollection.asme.org/energyresources

Selected Aspects of Performance of Organic Rankine Cycles Incorporated Into Bioenergy With Carbon Capture and Storage Using Gasification of Sewage Sludge

Kamil Stasiak[1]
Faculty of Mechanical Engineering and Ship Technology,
Institute of Energy,
Gdańsk University of Technology,
Narutowicza 11/12,
Gdansk 80-233, Poland
e-mail: kamil.stasiak@pg.edu.pl

Paweł Ziółkowski
Faculty of Mechanical Engineering and Ship Technology,
Institute of Energy,
Gdańsk University of Technology,
Narutowicza 11/12,
Gdansk 80-233, Poland
e-mail: pawel.ziolkowski1@pg.edu.pl

Dariusz Mikielewicz
Faculty of Mechanical Engineering and Ship Technology,
Institute of Energy,
Gdańsk University of Technology,
Narutowicza 11/12,
Gdansk 80-233, Poland
e-mail: dariusz.mikielewicz@pg.edu.pl

The study aims to investigate the application of the organic Rankine cycle (ORC) in the bioenergy with carbon capture and storage (BECCS) using gasification of sewage sludge. The tool used in the investigation is the ASPEN PLUS *software with* REFPROP *property methods for calculating fluid properties. The reason for this study is that a detailed analysis of the proposed BECCS process flow diagram indicates that a certain amount of waste heat is available in the exhaust gas from the high-to-intermediate pressure gas turbine. Some of this energy can be used by applying expansion in a low-pressure turbine, optionally by applying regenerative water heating, which is then redirected to the combustion chamber, or finally by incorporating the ORC into the main cycle. For the ORC cycle, different configurations are studied, with regeneration and using different working fluids. For the highest efficiency of the cycle, the regenerative heating of high-pressure water is applied and a suitable ORC working fluid with optimal saturation parameters and mass flow is selected. Such modified proposed BECCS power plant hybrid systems with ORC are compared to the reference case with lower pressure expansion. A study of the heat duty and temperature distribution in heat exchangers is carried out. Five ORC fluids were investigated, namely ethanol, refrigerants R236ea, R245fa, R1233zd(E), and water, which gave a net efficiency of the whole power plant of 39.71%, 40.02%, 40.26%, 40.34%, and 39.35% respectively, while the proposed BECCS reference case gave 38.89%.* [DOI: 10.1115/1.4064196]

Keywords: energy conversion/systems, energy from biomass, energy systems analysis, heat energy generation/storage/transfer, power (co-) generation

1 Introduction

Sewage sludge is one of the most abundant energy sources for perspective use in technologies for the production of useful energy in the form of electricity, heat, and others. The most promising ones are those that convert thermal energy into electricity. Another incentive to convert sewage sludge into electricity is that various legal restrictions prohibit its use as fertilizer, hence new ways of utilizing it should be sought [1]. One such solution is to convert sewage sludge by gasification to syngas and produce electricity. At the receiving end of this technology is the process of CO_2 capture, which leads to the idea of a cycle with a positive impact on the environment. Such an arrangement has already been presented in authors' earlier publications [2–6], and whole of the issues of the new technology in Ref. [7].

Organic Rankine cycle (ORC) is a type of Rankine cycle that uses a low-boiling temperature working fluid that allows waste heat to be recovered at lower temperatures. Thus, despite their lower efficiency, they can recover waste heat from sources otherwise unavailable to conventional Rankine steam cycles. An example of a simple ORC process flow diagram (PFD) is shown in Fig. 1. It consists of four main devices through which the working fluid flows in a closed loop in one direction, respectively: vapor turbine T-ORC with generator G ~, ORC condenser cooled by low-temperature source (LTS), ORC pump (P_{ORC}), and finally there is a ORC regenerative heat exchanger and evaporator (RHE_{ORC}). The working fluid is first pressurized, then evaporated in RHE_{ORC}, and the vapor is then expanded in a turbine to drive the generator. Finally, the expanded vapor is condensed and cooled, returning to the beginning, and closing the loop.

One of the aspects to be considered when selecting the working fluid in ORC systems is its operating temperature and the conditions

[1]Corresponding author.

Contributed by the Advanced Energy Systems Division of ASME for publication in the JOURNAL OF ENERGY RESOURCES TECHNOLOGY. Manuscript received June 15, 2023; final manuscript received October 6, 2023; published online January 9, 2024. Assoc. Editor: Wojciech Stanek.

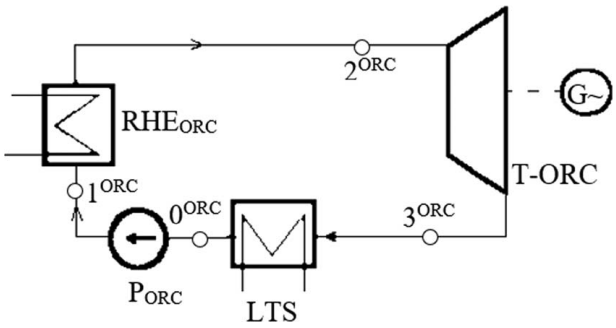

Fig. 1 Simple ORC process flow diagram

under which the working fluid will be used [8]. There are known works concerning both on the ORC systems with several hundreds of megawatt electric and micro combined heat and power (micro-CHP) plants adapted to the needs of prosumers, but the common feature is the consideration of several fluids adapted to the specific conditions of the energy system [9–11]. Another issue is the size of the unit, as the introduction of the ORC working fluid is very often associated with the compactness of the system, and sometimes the low-temperature part of the cycle is even replaced by a low-boiling fluid unit [12,13]. As literature studies show, the ORC cycle can be a bottoming cycle to a supercritical steam cycle [12,13], a fuel cell [14], or a simple Brayton cycle [15,16].

Motivation for introducing an ORC cycle into the proposed bioenergy with carbon capture and storage (BECCS) using gasification of sewage sludge (aka negative CO_2 power plant (nCO_2PP) system) is the fact that cycles with CO_2 capture require the management of a large amount of waste heat. In general, there are three main technologies for CO_2 capture, namely post-combustion [17,18], pre-combustion [19], and oxy-combustion [20], and therefore such waste heat is associated with various effects, including: compression and cooling of CO_2 [21], gasification of the fuel and its subsequent cooling [22], production of oxygen in cryogenic stations [23,24]. Examples of the use of ORCs for waste heat recovery can be found in various directions, but the most common is the production of electricity for the needs of a specific company. Electricity produced in this way reduces the operating costs of a company and is increasingly being used to meet the needs of production plants, where the use of the heat from: the chemical industry [25], petrochemical industry [26], cement factory processes [27], or simply from flue gases [28] should be mentioned. The process is often determined by the temperatures at which the working fluid for the turbine is directed, so it is necessary to distinguish between ranges such as low temperature [29], mid-range, and high temperature [30]. In addition, the ORC can be combined with an internal combustion engine [31] or a diesel engine [32]. Another aspect is the use of waste heat in ORC for the simultaneous production of electricity and heat in cogeneration [33,34], or electricity and refrigerant/air conditioning [35]. All these aspects make it worth considering a hybrid system combining the advantages of nCO_2PP and ORC cycles.

2 Low Temperature Potential for nCO_2PP

2.1 Primary Option With Spray-Ejector Condenser Versus nCO_2PP With Organic Rankine Cycle. The PFD of proposed BECCS is shown in Fig. 2. The BECCS using gasification of sewage sludge (aka nCO_2PP) is equipped with three key devices, namely: the high-temperature gasification reactor (R), the wet combustion chamber (WCC), and the spray-ejector condenser (SEC) [4]. The end of electrical energy generation in nCO_2PP, where key changes have been made, is highlighted by the dotted line. In the proposed configuration of BECCS, the GT^{bap} turbine is applied for the low-pressure electrical energy generation. The nCO_2PP reference case [2] employs the SEC to condense the steam in a direct condensation process and create a vacuum analogous to condensation in steam turbine cycles. The HE1 cools the exhaust gases before the SEC and heats water fed to the WCC [4].

The PFD of nCO_2PP after modification with ORC as an alternative to low-pressure expansion is presented in Fig. 3. ORC has been proposed as a novelty instead of low-pressure condensation and expansion. In this solution, heat exchanger HE1 receives energy from exhaust gases with a pressure of 1 bar, however, this process occurs significantly in higher temperature. Therefore, the ORC system is introduced to generate electricity as an alternative to GT^{bap} and at the same time utilize the low-temperature heat

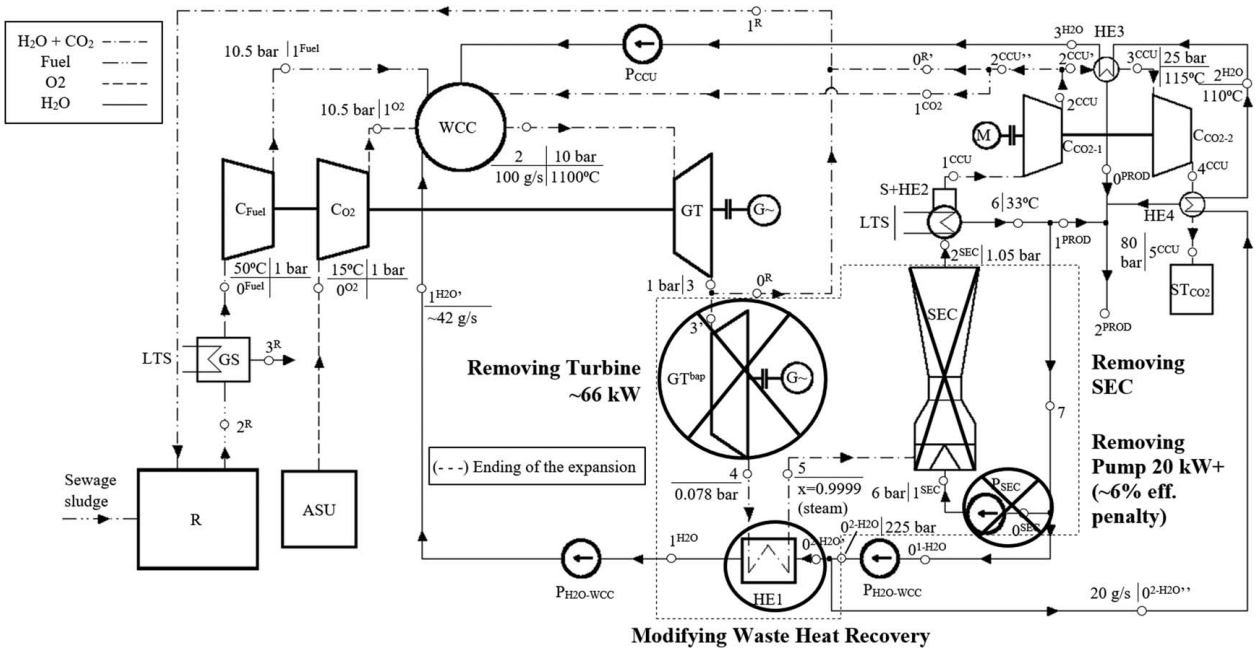

Fig. 2 PFD of proposed BECCS using gasification of sewage sludge—SEC low-pressure expansion, with highlighted modifications [2,4]

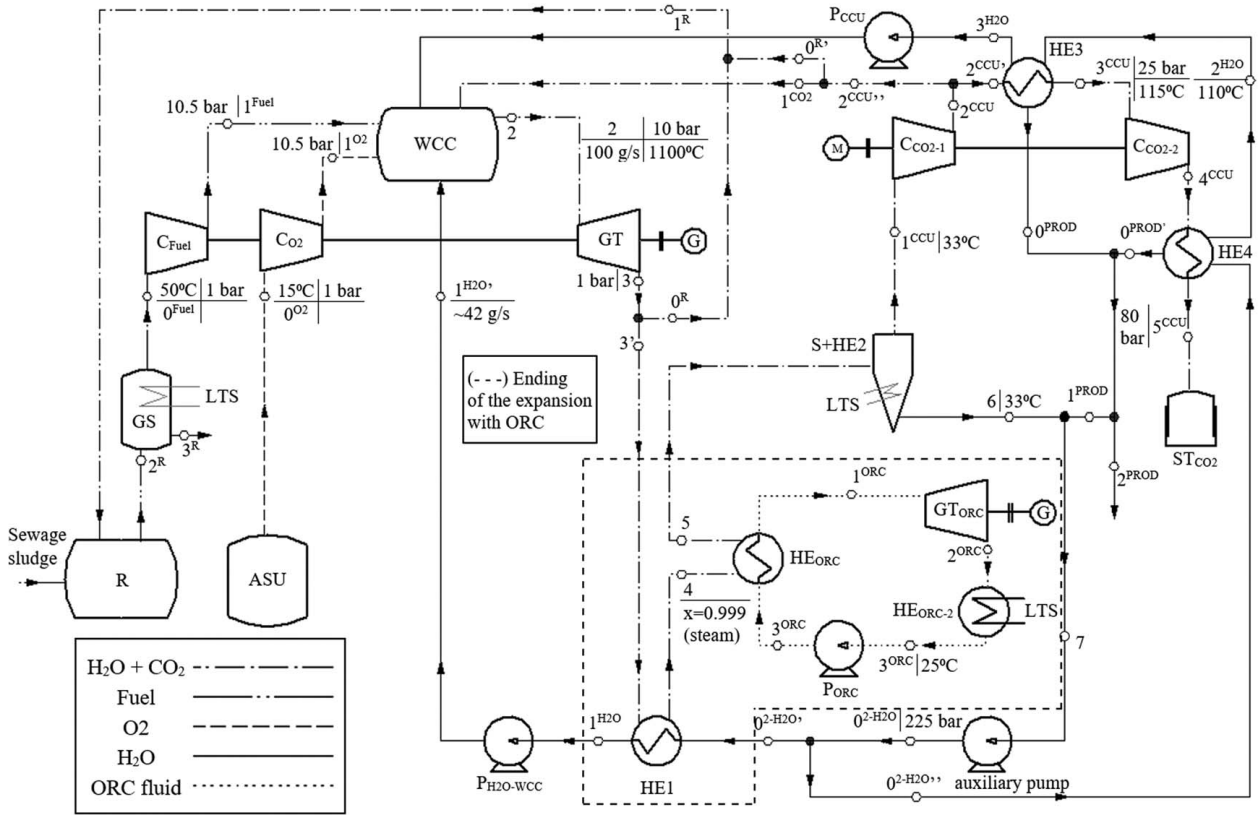

Fig. 3 Hybrid nCO$_2$PP PFD after modification with ORC as an alternative to low-pressure expansion [36]

unused in the SEC. The last exchanged device here is the centrifugal cyclone condenser to condense and separate the CO_2, which replaces the spray-ejector condenser. It should be noted that different condensers can be used for this purpose, for example, a spray condenser with optional gas injection to liquid.

2.2 Overview of Heat Duty and Temperature Distribution. Selected results for methane-fueled nCO$_2$PP are presented in the overview. The heat input of HE1 for different flue gas temperatures from the WCC is shown in Fig. 4. The 500 °C result differs from the others because HE1 is not used due to the low temperature of the flue gas after the turbine. The temperature distribution of HE1 for two different WCC exhaust temperatures of 1100 °C is shown in Fig. 5. From Fig. 5, it can be seen that at 1100 °C from the WCC there is no waste heat left to be used, although there is a high power consumption of the SEC pump as shown in Fig. 6, so the incorporation of the ORC instead of the SEC with turbine operating below ambient pressure can be treated as an alternative expansion. The motive fluid injected into the SEC is driven by the pump, which consumes power. The bar graphs in Fig. 6, showing the power consumption of this pump, are presented in two variants for each WCC temperature configuration, namely the optimistic assumption that all steam is condensed in the mixing chamber of the SEC, resulting in a lower motive fluid water flow, but the non-optimistic assumption that 25% of the steam is still not condensed in the mixing chamber (the optimistic assumption is used for all other calculations except this graph). Sufficient motive fluid water must be supplied to entrain all the CO_2, assuming that all the steam in this exhaust is condensed immediately. For example, the water flowrate would have to be reduced if the water content in the exhaust were higher (e.g., higher H_2 content in the syngas fuel) or the water flowrate would have to be increased if the CO_2 content in the exhaust were higher (e.g., due to a higher CO and CO_2 content in the syngas fuel). Under this assumption, the motive fluid water required by the SEC is largely dependent on the volume flowrate of CO_2

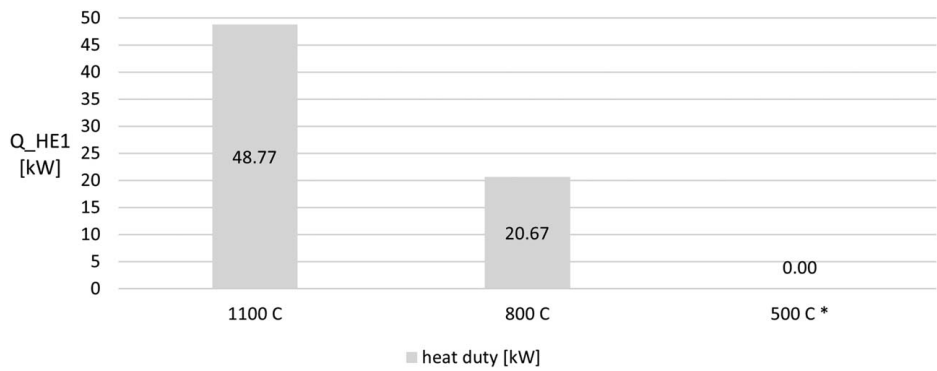

Fig. 4 Heat duty of HE1 based on nCO$_2$PP fueled by methane (without ORC incorporation)

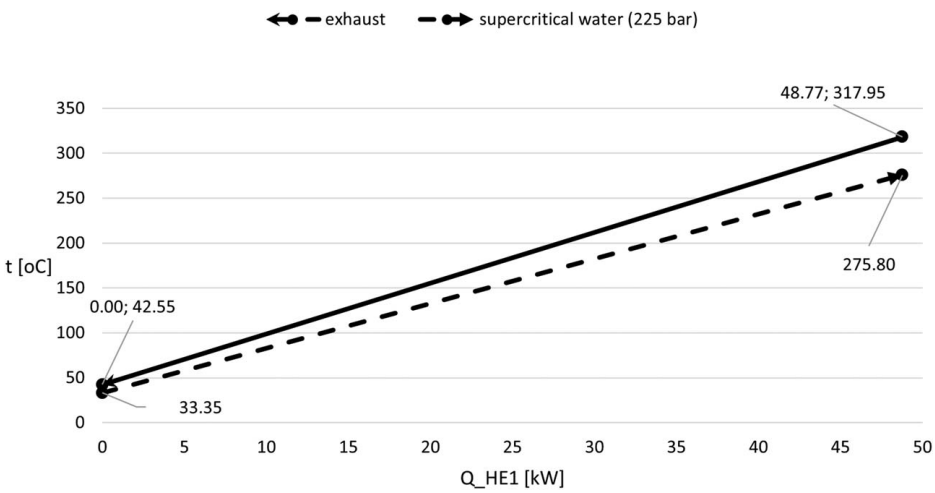

Fig. 5 Temperature distribution in HE1 based on nCO_2PP at the temperature of 1100 °C from WCC fueled by methane (without ORC incorporation)

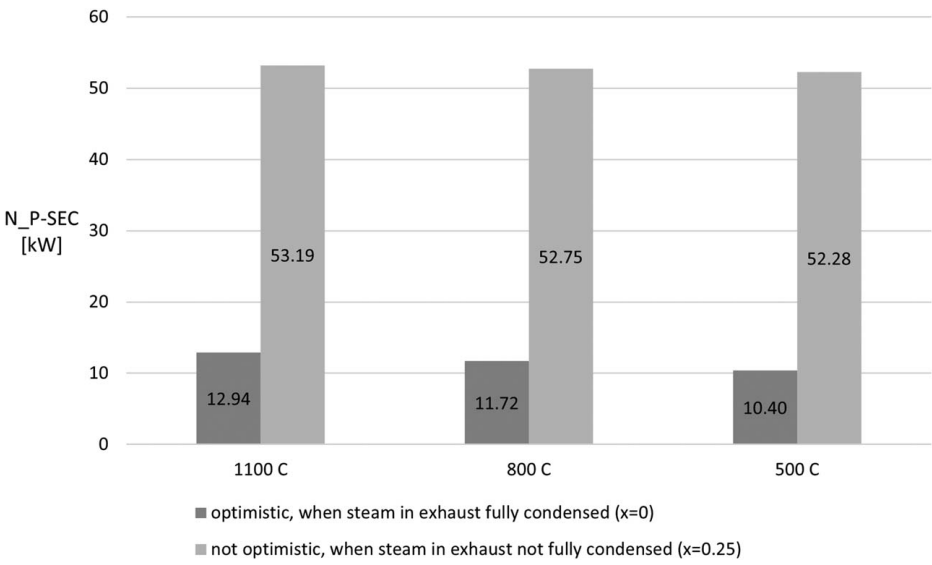

Fig. 6 SEC pump power consumption based on methane 10 bar, 100 g/s

vapor in the exhaust gas. Another important note for ORC incorporation is that while the nCO_2PP vacuum would be raised to ambient, an ORC evaporator would operate as a CO_2-gas-steam condenser instead of the SEC with the HE2 heat duty shown in Fig. 7.

3 Methodology

The calculations are performed using the ASPEN PLUS process flow simulator based on REFPROP. Data on key thermodynamic assumptions and values at selected nodal points are given in Table 1, while Table 2 summarizes the internal mechanical efficiency values for the modeled equipment. The most accurate equations of state found in the literature are used in the simulation and are listed in Table 3. Several ORC working fluids are investigated, namely ethanol, R236ea, R245fa, R1233zd(E), and water. The sensitivity analysis of the net power plant efficiency is performed by varying the ORC fluid pressure. The highest efficiency ORC configurations are obtained by fitting ORC temperature lines to the exhaust heat gas by finding the optimum ORC mass flowrate for a given optimum ORC fluid pressure while maintaining a pinch-point temperature difference of 5 K in the heat exchanger. The temperature distribution in the heat exchangers is obtained from their zone analysis results.

3.1 Organic Rankine Cycle Fluid Selection. The selection of the ORC fluid depends on required factors such as required thermodynamic properties, cost, flammability, toxicity, and environmental impact [50]. In the case of this work, a subcritical configuration of ORC has been considered and the selected fluids feature these requirements in a different extent. However, environmental impact is a favored factor due to regulations as well as the objective of the negative CO_2 power plant, needless to say this factor is positively correlated with the cost related to the global warming impact of a fluid [5]. In terms of thermodynamic properties, it is preferred that the ORC fluid temperature in the initial heating and saturation zones, which depend on specific and latent heat capacities, is well matched to the waste heat source temperature in order to utilize most of the available heat. For any working fluid, efficient heat exchanger design is critical for ORC performance [8].

Ethanol is an organic compound with a low boiling point, low toxicity, and environmental safety and is therefore recommended for domestic use; however it is a flammable fluid. Water is a

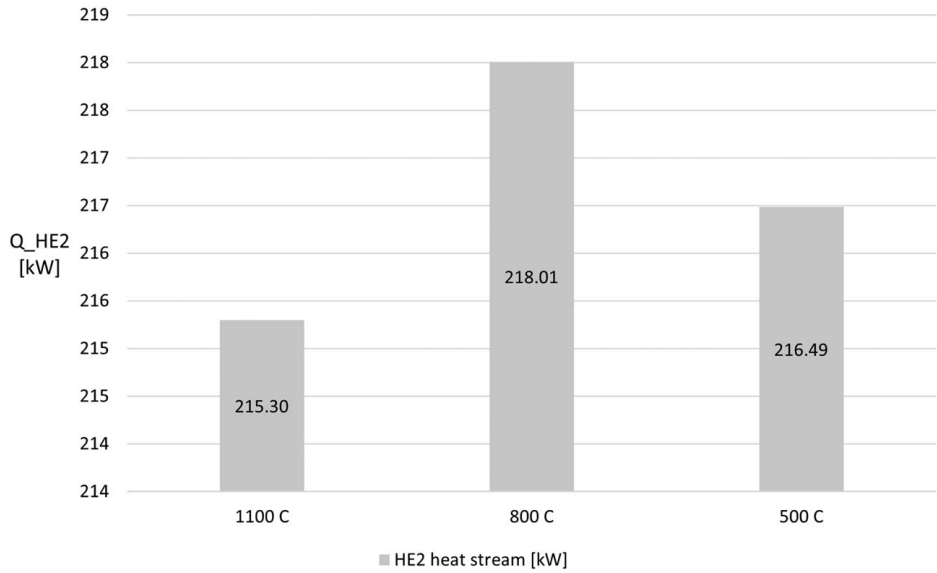

Fig. 7 SEC HE2 condensate cooler heat duty based on methane 10 bar, 100 g/s (optimistic)

Table 1 Basic data adopted for thermodynamic analyses

Parameter	Symbol	Unit	Value
Fuel	Syngas from sewage sludge: 9.3 vol% CO, 46.8% H_2, 13.9% CH_4, 26.4% CO_2, and 3.5% C_3H_8		
Working fluid	Gas-steam ($CO_2 + H_2O$)		
CO_2 capture technology	Oxy-combustion		
Temperature exhaust after WCC (before GT)	t_2	°C	1100
Mass flow of the exhaust gas from the WCC	$\dot{m}_2$	g/s	100
Exhaust pressure after WCC	p_2	bar	10
Oxygen-fuel ratio in WCC	λ	—	1
Initial fuel temperature	t_{fuel}	°C	50
Initial oxygen temperature	t_{O_2}	°C	15
Syngas fuel pressure before C_{fuel} compressor	p_{0-fuel}	bar	1
Oxygen pressure before CO_2 compressor	p_{0-O_2}	bar	1
Fuel to WCC pressure loss factor	δ_{fuel}	—	0.05
Oxygen to WCC pressure loss factor	δ_{O_2}	—	0.05
Regenerative water pressure to WCC	p_{1-H_2O}	bar	225
Heat exchangers pinch-point temperature difference	ΔT_{p-p}	K	5
Exhaust vapor quality after HE1	x_5	—	0.999
CO_2 pressure after compressor C_{CCU1}	p_{2-CCU}	bar	25
CO_2 pressure after compressor C_{CCU2}	p_{4-CCU}	bar	80
H_2O temperature after HE4	t_{2-H_2O}	°C	110
CO_2 temperature after HE3	t_{3-CCU}	°C	115
Water vapor from separator in 1^{CCU} mixed with CO_2 vapor	—	%	100% humid
Pressure after GT^{bap}, without ORC	p_4	bar	0.078
Pressure after GT, when ORC is incorporated	p_3	bar	1
Temperature of the waste exhaust heat	t_4	°C	96.8
Temperature of the waste exhaust heat, after separator + HE2 with LTS	t_6	°C	33
ORC lower temperature	t_{3-ORC}	°C	25
ORC working fluid	Ethanol, R236ea, R245fa, R1233zd(E), and water		

cheap and widely available fluid, although it is chosen for comparison in this work due to its industrial use. The refrigerants R236ea, R245fa, and R1233zd(E) have good thermodynamic properties to obtain optimal initial temperature ranges, are non-flammable and have low toxicity, although R236ea and R245fa are harmful to the environment, R236ea is also expensive, while R1233zd(E) is a new cheaper refrigerant that is also environmentally friendly.

3.2 Definitions of Efficiency and Power. The net power output is defined as

$$N_{net} = N_t - N_{cp} + N_{t-ORC}\ (kW) \quad (1)$$

in which N_t represents the power of the gas turbines, N_{cp} includes the sum of the power consumption of the auxiliary working devices, and N_{t-ORC} defines the power output of the ORC cycle.

$$N_{cp} = N_{C-Fuel} + N_{C-O_2} + N_{C-CO_2-1} + N_{C-CO_2-2} + N_{P-H_2O} + N_{P-ORC}\ (kW) \quad (2)$$

in which N_{C-Fuel}, N_{C-O_2}, N_{C-CO_2-1}, N_{C-CO_2-2} represent required powers of compressor for fuel, oxygen, and carbon dioxide, respectively, on the other hand, N_{P-H_2O} and N_{P-ORC} specify required powers of pump for water supply and ORC cycle, respectively.

Table 2 Assumed internal efficiency and mechanical efficiency, omitting the efficiency of the generator

Internal efficiency	Symbol	Unit	Value
Turbine GT	η_{iGT}	—	0.89
Turbine GT^{bap}	$\eta_{iGT-bap}$	—	0.89
Turbine GT-ORC	$\eta_{iGT-ORC}$	—	0.89
Fuel compressor C_{fuel}	$\eta_{iC-fuel}$	—	0.87
Oxygen compressor CO_2	η_{iC-O_2}	—	0.87
Water pump P_{H_2O}	η_{iP-H_2O}	—	0.8
Water pump P_{SEC}	η_{iP-SEC}	—	0.8
Water pump P-ORC	η_{iP-ORC}	—	0.8
CO_2 compressor C_{CO_2-1}	η_{iC-CO_2-1}	—	0.87
CO_2 compressor C_{CO_2-2}	η_{iC-CO_2-2}	—	0.87
Mechanical efficiency for all devices	η_m	—	0.99

Overall (net) power plant efficiency

$$\eta_{net} = \frac{N_{net}}{LHV_{syngas} \cdot \dot{m}_{0-fuel}} (\%) \quad (3)$$

where LHV_{syngas} and $\dot{m}_{0-fuel}$ define the lower heating value of the gas produced in the gasifier and cleaned and dried in the scrubber and the mass flowrate of syngas.

3.3 Optimization Task Overview. For the optimization tasks during the simulation, the secant method is used for a single design specification, the Broyden method for combining multiple design specifications, the Wegstein method for tear streams, and the sequential quadratic programming (SQP) method for optimal point search. The secant method iteratively updates the two intersection points between an approximated secant line and the function until these points converge to a local amplitude [51]. The Broyden method is an extension of the secant method that iteratively approximates the Jacobian matrix [51]. The Wegstein method solves nonlinear equations iteratively by finding their roots by approximation [52]. The SQP method solves constrained nonlinear problems by updating the search direction of a constrained subproblem at each iteration [51].

The design specifications used in the simulation are as follows: WCC with constant combustion temperature of 1100 °C, WCC with constant mass flow of 100 g/s, ORC finding lower pressure related to 25 °C, ORC finding the highest efficiency saturation pressure related to boiling temperature, ORC mass flow for temperature difference at pinch point. The design specification for the WCC constant temperature of 1100 °C is solved by introducing water mass flow range, and WCC constant mass flow is obtained by applying fuel mass flow range, and also both design specifications are solved depending on each other. The ORC lower pressure of a fluid related to 25 °C is found by applying the pressure range. The design specification for the highest ORC efficiency is solved by applying the pressure range depending on the other design specification which is the mass flow at allowable temperature difference at the pinch point. For the sensitivity analysis of the ORC fluid saturation pressure or boiling temperature on the overall net efficiency of the power plant, the range of the ORC pump pressure is obtained while the design specification for finding the pressure is deactivated [50].

4 Results and Discussion of Calculations for Hybrid nCO$_2$PP With Organic Rankine Cycle

Due to the high heat recovery potential presented in the second chapter showing the temperature distribution in heat exchangers, ORC incorporation analysis is performed. In this modification, only the GT^{bap} turbine and SEC with its pump are deactivated, while the operation of the HE1 heat exchanger is changed by increasing its heating duty. The results from the reference case shown in Fig. 2 are added to the results table as the first column for comparison. The results for ORC integration based on PFD shown in Fig. 3 based on ORC fluids are added to all other columns, namely for water, ethanol, refrigerants R236ea, R245fa, and R1233zd(E). The temperature distribution results for all ORC fluids from Table 4 are shown in Figs. 8–12, which are on a logarithmic scale for better visualization. These figures show the maximized regenerative water heating for maximum power plant efficiency.

The results have been generated using ASPEN PLUS process simulation software. The results in the table have been adjusted to achieve maximum efficiency by modifying the ORC parameters. Each calculation was optimized to maintain an exhaust temperature of 1100 °C at a mass flow of 100 g/s and a pressure of 10 bar, and the fuel for the combustion chamber was syngas "Mixture 2" obtained from sewage sludge gasification (see Ref. [3]). A minimum temperature difference of 5 K was applied at the pinch points of the temperature distribution.

Table 4 shows the results comparing different configurations. First is the reference case nCO$_2$PP power plant with SEC and without ORC, next is the hybrid nCO$_2$PP with water as ORC working fluid, then there is ethanol as ORC fluid, the other is hybrid nCO$_2$PP with R236ea refrigerant as ORC working fluid, then there is hybrid nCO$_2$PP with R245fa refrigerant as ORC working fluid and the last one is R1233zd(E). In addition, each hybrid nCO$_2$PP result corresponds to the maximum overall net power plant efficiency obtained by adjusting the optimum ORC parameters.

4.1 Temperature Distribution for Different Cases With Organic Rankine Cycle Working Fluid. Figures 8–12 show logarithmic scale temperature distribution plots for heat exchangers

Table 3 Governing equations [37]

Flow type	Fluid short name	Chemical formula	Equation of state	Comments
Exhaust medium	Water	H_2O	Wagner and Pruß [38]	Steam tables
	Carbon dioxide	CO_2	Span and Wagner [39]	NIST standard
Syngas combustion	Oxygen	O_2	Schmidt and Wagner [40]	
	Methane	CH_4	Setzmann and Wagner [41]	
	Carbon monoxide	CO	Lemmon and Span [42]	
	Hydrogen	H_2	Leachman et al. [43]	
	Propane	C_3H_8	Lemmon et al. [44]	
ORC fluids	R236ea	$C_3H_2F_6$	Rui et al. [45]	
	R245fa	$C_3H_3F_5$	Akasaka et al. [46]	
	R1233zd(E)	$C_3H_2ClF_3$	Mondejar et al. [47]	
	Ethanol	C_2H_5OH	Schroeder et al. [48]	
Helmholtz mixing model			Kunz and Wagner [49]	ISO standard
ORC heat source final temperature evaluation			Mikielewicz and Mikielewicz [8]	Validation

Table 4 Results of different configurations

Parameter	Symbol	Unit	nCO_2PP reference case (with SEC, without ORC)	Hybrid nCO_2PP combined with ORC featuring				
				Water	Ethanol	R236ea	R245fa	R1233zd(E)
Water mass flow injection to WCC	$\dot{m}_{1-H_2O}$	g/s	63.11	69.20	69.20	69.20	69.20	69.20
Water mass flow in exhaust	$\dot{m}_{2-H_2O}$	g/s	76.91	80.70	80.70	80.70	80.70	80.70
CO_2 mass flow in exhaust	$\dot{m}_{2-CO_2}$	g/s	23.09	19.19	19.19	19.19	19.19	19.19
Exhaust temperature after regenerative water heat exchanger	t_4	°C	$35(t_5)$	96.82	96.82	96.82	96.82	96.82
Turbine power GT	N_{GT}	kW	90.45	92.68	92.68	92.68	92.68	92.68
Turbine power GT^{ORC}	N_{GT}	kW	65.78 as GT^{bap}	21.73	22.6	24.46	24.44	24.53
	$-ORC$							
Power for own needs	N_{cp}	kW	47.15	22.26	22.28	23.09	22.84	22.76
ORC boiling temperature	$t_{1-2\ ORC}$	°C	—	79.51	79.77	87.14	85.85	84.80
ORC/water mass flowrate	$\dot{m}_{ORC}$	g/s	—	64.95	173.8	959.6	805.7	817.0
Chemical energy rate of combustion	$\dot{Q}_{CC}$	kW	280.45	234.15	234.15	234.15	234.15	234.15
Net efficiency	η_{net}	%	38.89	39.35	39.71	40.02	40.26	40.34

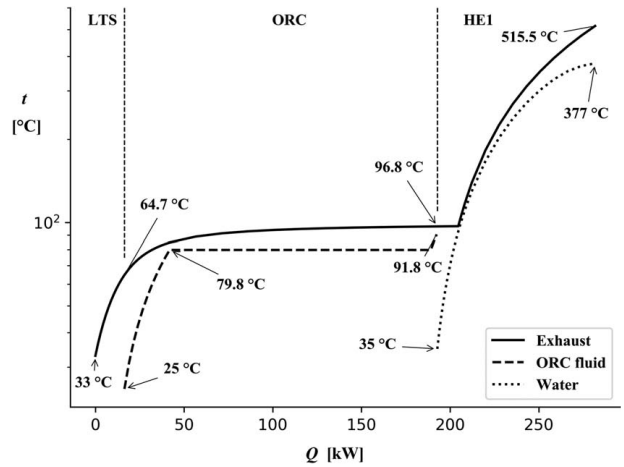

Fig. 8 Logarithmic scale of temperature distribution with ethanol as ORC fluid

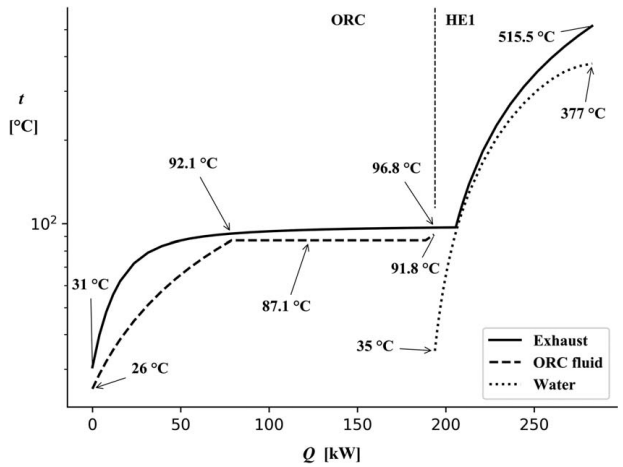

Fig. 10 Logarithmic scale of temperature distribution with R236ea as ORC fluid

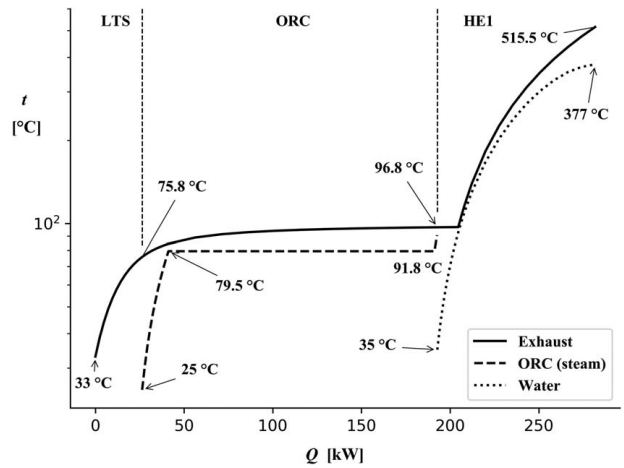

Fig. 9 Logarithmic scale of temperature distribution with steam as ORC fluid

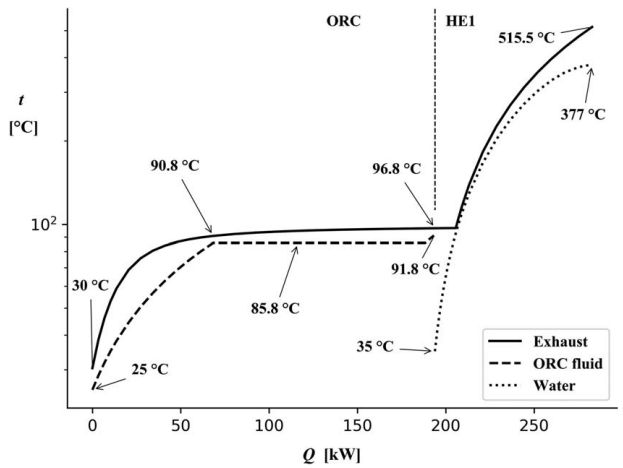

Fig. 11 Logarithmic scale of temperature distribution with R245fa as ORC fluid

exchanging heat between the exhaust gas temperature line and the ORC cooling fluid and pressurized water directed to the WCC temperature lines. The exhaust gas temperature is shown as a solid line, the ORC fluid as a dashed line on the left, and the pressurized water regeneratively heated by the hot waste heat exhaust gas before being fed to the WCC as a dotted line. In addition, each graph is divided into two or three segments, which are described at the top of each graph, where LTS is used to sub-cool the remaining exhaust heat to 33 °C, ORC is the heat exchange taking place in the HE-ORC evaporator, and HE1 corresponds to the heat exchange in the regenerative heat exchanger HE1 between the exhaust gas and the pressurized water fed to the WCC.

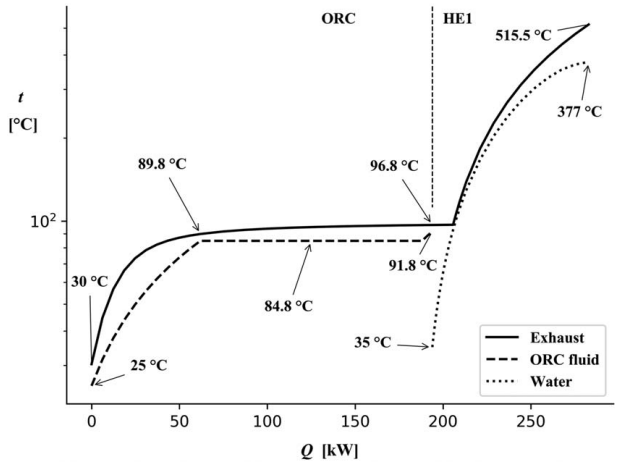

Fig. 12 Logarithmic scale of temperature distribution with R1233zd(*E*) as ORC fluid

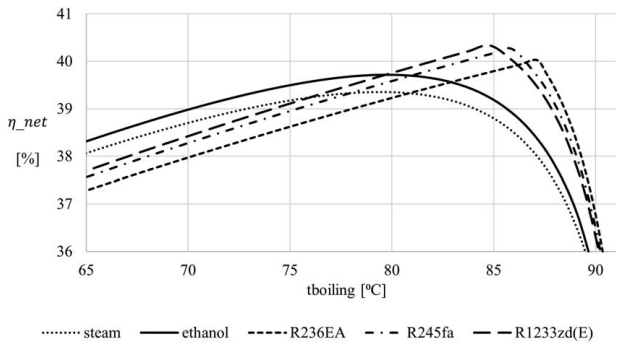

Fig. 13 Sensitivity analysis for steam, ethanol, R236ea, R245fa, and R1233zd(*E*) as ORC fluids

4.2 Sensitivity Analysis of Net Power Plant Efficiency to Varying Organic Rankine Cycle Working Fluid Boiling Temperature. In order to maximize the overall efficiency of the power plant, the maximum amount of waste heat must be effectively utilized. Two factors play a crucial role in maximizing efficiency on the ORC side, namely pressure and mass flow. Pressure corresponds to the boiling point temperature and therefore a correct value of this parameter allows a better adaptation to the temperature line of both condensing and cooling exhaust gas in the temperature distribution. The mass flow of the ORC fluid allows to effectively maximize the heat flow at the given level of the ORC boiling temperature. Figure 13 shows the optimization task for the optimum boiling temperature point, which gives the maximum overall net efficiency of the power plant.

The graph in Fig. 13 shows the sensitivity analysis of the net power plant efficiency of nCO_2PP with ORC to varying boiling temperature of ORC fluid. The efficiency lines for refrigerants are asymptotic, while those for ethanol and steam are parabolic. Also, the efficiency lines in this sensitivity analysis for the refrigerants R236ea, R245fa, and R1233zd(E) bend sharply at 87.1 °C, 85.8 °C, and 84.8 °C, respectively, because higher boiling temperatures violate the minimum temperature difference of 5 K at the pinch point in the heat exchanger versus the somewhat fixed flue gas temperature, so the ORC mass flow is greatly reduced at higher boiling temperatures to maintain this temperature difference. This does not occur for steam and ethanol ORC fluids due to different thermodynamic properties for the initial temperature zones, which can be seen as a different shape of the ORC fluid temperature line in Figs. 8–9 versus 10–12, as refrigerants have a more sloped line that shifts to the left, closer to the exhaust line, at higher boiling temperatures, which can be addressed to different specific to latent heat ratios, while the working fluid mass flow is different for the compared fluids. These characteristics also allow R236ea, R245fa, and R1233zd(E) fluids to utilize the given waste heat in the lower temperature range of the exhaust gas, which was not the case for ethanol or steam where subcooling from a lower temperature source was used to reduce the waste heat exhaust temperature to 33 °C.

Steam as ORC working fluid, represented by the dotted line, achieves the maximum efficiency of 39.35% at a boiling temperature of 79.5 °C (saturation pressure of 0.46 bar) and a mass flow of 64.95 g/s, resulting in a power output of 21.73 kW from the ORC turbine.

Ethanol as ORC working fluid shows the highest overall net power plant efficiency of 39.71% for the boiling temperature of 80.1 °C (saturation pressure of 1.08 bar), 173 g/s giving 22.6 kW ORC turbine brake power, this sensitivity analysis efficiency line is represented by a solid line.

R236ea refrigerant as ORC working fluid showed the highest efficiency for the boiling temperature of 87.1 °C (11.84 bar), 966 g/s giving 24.5 kW ORC turbine brake power and maximum overall hybrid net efficiency of 40.02%, this sensitivity analysis line is represented by a dashed line.

R245fa refrigerant as ORC working fluid showed the highest efficiency for 85.8 °C boiling temperature 9.11 bar, 806 g/s giving 24.4 kW ORC turbine brake power and maximum overall hybrid net efficiency of 40.26%, this sensitivity analysis efficiency line is represented by the dashed dotted line.

The use of R1233zd(E) as the ORC working fluid gave the highest efficiency of 40.34% at a boiling temperature of 84.8 °C (7.38 bar) at a mass flow of 817 g/s giving 24.53 kW ORC turbine power, the results of this fluid are represented by the long-dashed line on the graph.

5 Conclusions and Perspectives

(1) The exhaust mixture of CO_2 and H_2O, below the boiling temperature of water, has the twofold characteristics of gradually decreasing its temperature on cooling, while the steam is condensed.
(2) The refrigerants R236ea, R245fa, and R1233zd(E) are more suitable as ORC working fluids than ethanol or steam due to a different ratio of specific to latent heat capacity, resulting in a different shape of the temperature lines in the initial heating zones, which means a better adaptation of the temperature distribution along the heat exchanger to the given process conditions.
(3) ORC can be further optimized, e.g., by selecting the best working fluid and according to changing flue gas conditions (changing syngas fuel conditions), using waste heat from carbon capture or gasification units and applying differential condensation of CO_2-steam-gas in the ORC heat exchanger. Essentially, the way to increase the ORC higher temperature should be explored.
(4) ORC turbine output can be used for nCO_2PP auxiliary power consumption as the values are comparable.
(5) A significant part of the net efficiency loss in the original low-pressure expansion concept comes from the SEC pump high power consumption to drive large amounts of motive fluid water to the SEC and traditional vacuum steam condenser would not be a solution for a such CO_2--gas-steam mixture, giving opportunity for ORC modifications without low-pressure exhaust expansion. However, in this case, a new way of separating CO_2 from water has to be proposed for the new hybrid cycle. This is a new research issue not developed in this paper.
(6) The ORC combined hybrid plant achieves a similar or better net efficiency than the reference concept nCO_2PP with low-pressure expansion (if the power consumption of the SEC pump is included). ORC with ethanol gave a net efficiency

of 39.71%, reference nCO$_2$PP concept 38.89%, while ORC with refrigerants gave even higher net efficiencies R236ea 40.02%, R245fa 40.26%, and R1233zd(E) 40.34%.

Due to the high heat recovery potential presented in this paper, which shows the temperature distribution in heat exchangers and SEC, the organic Rankine cycle is also considered as an alternative to the low-pressure expansion turbine with water, ethanol, R236ea, R245fa or R1233zd(E) as working fluids. R1233zd(E) fluid yields the highest efficiency and also has characteristics such as environmental friendliness, low toxicity, and non-flammability at a relatively low cost compared to other fluids studied.

A hybrid system integrating the advantages of nCO$_2$PP and the ORC cycle is a promising solution and modifications are possible, but the main advantage is that the ORC cycle can be introduced as a component to provide electrical power in the lower temperature range. Similar solutions [12,13] using steam condensation to drive the ORC have been developed for supercritical coal-fired units with favorable results, providing further confirmation of the research direction taken.

Acknowledgment

The research leading to these results has been funded by Norway Grants 2014–2021 via the National Centre for Research and Development. This research has been prepared within the project "Negative CO_2 Emission Gas Power Plant"—NOR/POLNORCCS/NEGATIVE-CO_2-PP/0009/2019-00, which is co-financed by the "Applied Research" Programme under the Norwegian Financial Mechanisms 2014–2021 POLNOR CCS 2019—Development of CO_2 capture solutions integrated in power and industrial processes.

Conflict of Interest

There are no conflicts of interest.

Data Availability Statement

The authors attest that all data for this study are included in the paper.

References

[1] United Nations, 2016, The Paris Agreement | UNFCCC,
[2] Ziółkowski, P., Madejski, P., Amiri, M., Kuś, T., Stasiak, K., Subramanian, N., Pawlak-Kruczek, H., Badur, J., Niedźwiecki, Ł, and Mikielewicz, D., 2021, "Thermodynamic Analysis of Negative CO2 Emission Power Plant Using Aspen Plus, Aspen Hysys, and Ebsilon Software," Energies, **14**(19), p. 6304.
[3] Ziółkowski, P., Badur, J., Pawlak-Kruczek, H., Stasiak, K., Amiri, M., Niedzwiecki, L., Krochmalny, K., Mularski, J., Madejski, P., and Mikielewicz, D., 2022, "Mathematical Modelling of Gasification Process of Sewage Sludge in Reactor of Negative CO2 Emission Power Plant," Energy, **244**(Part A), p. 122601.
[4] Ziółkowski, P., Stasiak, K., Amiri, M., and Mikielewicz, D., 2023, "Negative Carbon Dioxide Gas Power Plant Integrated With Gasification of Sewage Sludge," Energy, **262**(Part B), p. 125496.
[5] Ziółkowski, P., Pawlak-kruczek, H., Madejski, P., Bukowski, P., Ochrymiuk, T., Stasiak, K., Amiri, M., Niedzwiecki, L., and Mikielewicz, D., 2022, "Thermodynamic, Ecological, and Economic Analysis of Negative CO2 Emission Power Plant Using Gasified Sewage Sludge," 2nd International Conference on Negative CO2 Emissions, Göteborg, Sweden, June 14–17.
[6] Stasiak, K., Ziółkowski, P., and Mikielewicz, D., 2020, "Carbon Dioxide Recovery Skid," Prog. Petrochem. Sci., **3**(4), pp. 362–364.
[7] 2023, "Negative CO2 Emission Gas Power Plant Project Site." nco2pp.com, Accessed February 26, 2023.
[8] Mikielewicz, D., and Mikielewicz, J., 2010, "A Thermodynamic Criterion for Selection of Working Fluid for Subcritical and Supercritical Domestic Micro CHP," Appl. Therm. Eng., **30**(16), pp. 2357–2362.
[9] Dai, Y., Wang, J., and Gao, L., 2009, "Parametric Optimization and Comparative Study of Organic Rankine Cycle (ORC) for Low Grade Waste Heat Recovery," Energy Convers. Manage., **50**(3), pp. 576–582.
[10] Mikielewicz, D., and Mikielewicz, J., 2014, "Analytical Method for Calculation of Heat Source Temperature Drop for the Organic Rankine Cycle Application," Appl. Therm. Eng., **63**(2), pp. 541–550.
[11] Wajs, J., Mikielewicz, D., Bajor, M., and Kneba, Z., 2016, "Experimental Investigation of Domestic Micro-CHP Based on the Gas Boiler Fitted With ORC Module," Arch. Thermodyn., **37**(3), pp. 79–93.
[12] Ziółkowski, P., Kowalczyk, T., Kornet, S., and Badur, J., 2017, "On Low-Grade Waste Heat Utilization From a Supercritical Steam Power Plant Using an ORC-Bottoming Cycle Coupled With Two Sources of Heat," Energy Convers. Manage., **146**, pp. 158–173.
[13] Mikielewicz, D., Wajs, J., Ziółkowski, P., and Mikielewicz, J., 2016, "Utilisation of Waste Heat From the Power Plant by Use of the ORC Aided With Bleed Steam and Extra Source of Heat," Energy, **97**, pp. 11–19.
[14] Wang, H., Zhao, H., and Zhao, Z., 2021, "Thermodynamic Performance Study of a New SOFC-CCHP System With Diesel Reforming by CLHG to Produce Hydrogen as Fuel," Int. J. Hydrog. Energy, **46**(44), pp. 22956–22973.
[15] Kowalczyk, T., Badur, J., and Ziółkowski, P., 2020, "Comparative Study of a Bottoming SRC and ORC for Joule–Brayton Cycle Cooling Modular HTR Exergy Losses, Fluid-Flow Machinery Main Dimensions, and Partial Loads," Energy, **206**, p. 118072.
[16] Nami, H., Ertesvåg, I. S., Agromayor, R., Riboldi, L., and Nord, L. O., 2018, "Gas Turbine Exhaust Gas Heat Recovery by Organic Rankine Cycles (ORC) for Offshore Combined Heat and Power Applications—Energy and Exergy Analysis," Energy, **165**(Part B), pp. 1060–1071.
[17] Madejski, P., Chmiel, K., Subramanian, N., and Kus, T., 2022, "Methods and Techniques for CO2 Capture: Review of Potential Solutions and Applications in Modern Energy Technologies," Energies, **15**(3), pp. 887.
[18] Amrollahi, Z., Ystad, P. A. M., Ertesvåg, I. S., and Bolland, O., 2012, "Optimized Process Configurations of Post-Combustion CO2 Capture for Natural-Gas-Fired Power Plant—Power Plant Efficiency Analysis," Int. J. Greenh. Gas Control., **8**, pp. 1–11.
[19] Ertesvåg, I. S., Kvamsdal, H. M., and Bolland, O., 2005, "Exergy Analysis of a Gas-Turbine Combined-Cycle Power Plant With Precombustion CO2 Capture," Energy, **30**(1), pp. 5–39.
[20] Kotowicz, J., Job, M., and Brzęczek, M., 2020, "Thermodynamic Analysis and Optimization of an Oxy-Combustion Combined Cycle Power Plant Based on a Membrane Reactor Equipped With a High-Temperature Ion Transport Membrane ITM," Energy, **205**, pp. 117912.
[21] Bartela, Ł, Skorek-Osikowska, A., and Kotowicz, J., 2014, "Thermodynamic, Ecological and Economic Aspects of the Use of the Gas Turbine for Heat Supply to the Stripping Process in a Supercritical CHP Plant Integrated With a Carbon Capture Installation," Energy Convers. Manage., **85**, pp. 750–763.
[22] Vishwajeet, Pawlak-Kruczek, H., Baranowski, M., Czerep, M., Chorążyczewski, A., Krochmalny, K., Ostrycharczyk, M., et al., 2022, "Entrained Flow Plasma Gasification of Sewage Sludge–Proof-of-Concept and Fate of Inorganics," Energies, **15**(5), pp. 1–14.
[23] Aneke, M., and Wang, M., 2015, "Process Analysis of Pressurized Oxy-Coal Power Cycle for Carbon Capture Application Integrated With Liquid Air Power Generation and Binary Cycle Engines," Appl. Energy, **154**, pp. 556–566.
[24] Mehrpooya, M., and Zonouz, M. J., 2017, "Analysis of an Integrated Cryogenic Air Separation Unit, Oxy-Combustion Carbon Dioxide Power Cycle and Liquefied Natural Gas Regasification Process by Exergoeconomic Method," Energy Convers. Manage., **139**, pp. 245–259.
[25] Ozalp, N., 2009, "Utilization of Heat, Power, and Recovered Waste Heat for Industrial Processes in the U.S. Chemical Industry," ASME J. Energy Resour. Technol., **131**(2), p. 224011.
[26] Zhang, L., Pan, Z., Zhang, Z., Shang, L., Wen, J., and Chen, S., 2018, "Thermodynamic and Economic Analysis Between Organic Rankine Cycle and Kalina Cycle for Waste Heat Recovery From Steam-Assisted Gravity Drainage Process in Oilfield," ASME J. Energy Resour. Technol., **140**(12), p. 122005.
[27] Fergani, Z., Morosuk, T., and Touil, D., 2020, "Performances Optimization and Comparison of Two Organic Rankine Cycles for Cogeneration in the Cement Plant," ASME J. Energy Resour. Technol., **142**(2), p. 022001.
[28] Roge, N. H., Khankari, G., and Karmakar, S., 2022, "Waste Heat Recovery From Fly Ash of 210 MW Coal Fired Power Plant Using Organic Rankine Cycle," ASME J. Energy Resour. Technol., **144**(8), p. 082107.
[29] Ziviani, D., Beyene, A., and Venturini, M., 2014, "Design, Analysis and Optimization of a Micro-CHP System Based on Organic Rankine Cycle for Ultralow Grade Thermal Energy Recovery," ASME J. Energy Resour. Technol., **136**(1), p. 011602.
[30] Yan, D., Yang, F., Zhang, H., Xu, Y., Wang, Y., Li, J., and Ge, Z., 2022, "How to Quickly Evaluate the Thermodynamic Performance and Identify the Optimal Heat Source Temperature for Organic Rankine Cycles?," ASME J. Energy Resour. Technol., **144**(11), p. 112106.
[31] Jacobs, T. J., 2015, "Waste Heat Recovery Potential of Advanced Internal Combustion Engine Technologies," ASME J. Energy Resour. Technol., **137**(4), p. 042004.
[32] Yang, F., Cho, H., and Zhang, H., 2019, "Performance Prediction and Optimization of an Organic Rankine Cycle Using Back Propagation Neural Network for Diesel Engine Waste Heat Recovery," ASME J. Energy Resour. Technol., **141**(6), p. 062006.
[33] Micheli, D., Pinamonti, P., Reini, M., and Taccani, R., 2013, "Performance Analysis and Working Fluid Optimization of a Cogenerative Organic Rankine Cycle Plant," ASME J. Energy Resour. Technol., **135**(2), p. 021601.
[34] Pan, Z., Yan, M., Shang, L., Li, P., Zhang, L., and Liu, J., 2020, "Thermoeconomic Analysis of a Combined Natural Gas Cogeneration System With a Supercritical CO2 Brayton Cycle and an Organic Rankine Cycle," ASME J. Energy Resour. Technol., **142**(10), p. 102108.

[35] Khaliq, A., Kumar, R., and Dincer, I., 2009, "Exergy Analysis of an Industrial Waste Heat Recovery Based Cogeneration Cycle for Combined Production of Power and Refrigeration," ASME J. Energy Resour. Technol., **131**(2), p. 022402.
[36] Stasiak, K., Ziółkowski, P., and Mikielewicz, D., 2022, "Assessment, Optimisation and Working Fluid Comparison of Organic Rankine Cycle Combined With Negative CO2 Gas Power Plant System," 7th International Conference on Contemporary Problems of Thermal Engineering, Warsaw, Poland, Sept. 20–23, pp. 357–367.
[37] Huber, M. L., Lemmon, E. W., Bell, I. H., and McLinden, M. O., 2022, "The NIST REFPROP Database for Highly Accurate Properties of Industrially Important Fluids," Ind. Eng. Chem. Res., **61**(42), pp. 15449–15472.
[38] Wagner, W., and Pruß, A., 2002, "The IAPWS Formulation 1995 for the Thermodynamic Properties of Ordinary Water Substance for General and Scientific Use," J. Phys. Chem. Ref. Data, **31**(2), pp. 387–535.
[39] Span, R., and Wagner, W., 2009, "A New Equation of State for Carbon Dioxide Covering the Fluid Region From the Triple-Point Temperature to 1100 K at Pressures Up to 800 MPa," J. Phys. Chem. Ref. Data, **25**(6), pp. 1509–1596.
[40] Schmidt, R., and Wagner, W., 1985, "A New Form of the Equation of State for Pure Substances and Its Application to Oxygen," Fluid Phase Equilib., **19**(3), pp. 175–200.
[41] Setzmann, U., and Wagner, W., 2009, "A New Equation of State and Tables of Thermodynamic Properties for Methane Covering the Range From the Melting Line to 625 K at Pressures Up to 1000 MPa," J. Phys. Chem. Ref. Data, **20**(6), pp. 1061–1155.
[42] Lemmon, E. W., and Span, R., 2006, "Short Fundamental Equations of State for 20 Industrial Fluids," J. Chem. Eng. Data, **51**(3), pp. 785–850.
[43] Leachman, J. W., Jacobsen, R. T., Penoncello, S. G., and Lemmon, E. W., 2009, "Fundamental Equations of State for Parahydrogen, Normal Hydrogen, and Orthohydrogen," J. Phys. Chem. Ref. Data, **38**(3), pp. 721–748.
[44] Lemmon, E. W., McLinden, M. O., and Wagner, W., 2009, "Thermodynamic Properties of Propane. III. A Reference Equation of State for Temperatures From the Melting Line to 650 K and Pressures Up to 1000 MPa," J. Chem. Eng. Data, **54**(12), pp. 3141–3180.
[45] Rui, X., Pan, J., and Wang, Y., 2013, "An Equation of State for the Thermodynamic Properties of 1,1,1,2,3,3-Hexafluoropropane (R236ea)," Fluid Phase Equilib., **341**, pp. 78–85.
[46] Akasaka, R., Zhou, Y., and Lemmon, E. W., 2015, "A Fundamental Equation of State for 1,1,1,3,3-Pentafluoropropane (R-245fa)," J. Phys. Chem. Ref. Data, **44**(1), p. 013104.
[47] Mondéjar, M. E., Mclinden, M. O., and Lemmon, E. W., 2015, "Thermodynamic Properties of Trans-1-Chloro-3,3,3-Trifluoropropene (R1233zd(E)): Vapor Pressure, (p, ρ, T) Behavior, and Speed of Sound Measurements, and Equation of State," J. Chem. Eng. Data, **60**(8), pp. 2477–2489.
[48] Schroeder, J. A., Penoncello, S. G., and Schroeder, J. S., 2014, "A Fundamental Equation of State for Ethanol," J. Phys. Chem. Ref. Data, **43**(4), pp. 043102.
[49] Kunz, O., and Wagner, W., 2012, "The GERG-2008 Wide-Range Equation of State for Natural Gases and Other Mixtures: An Expansion of GERG-2004," J. Chem. Eng. Data, **57**(11), pp. 3032–3091.
[50] Macchi, E., and Astolfi, M., 2017, *Organic Rankine Cycle (ORC) Power Systems*, Elsevier, New York.
[51] Nocedal, J., and Wright, S. J., 2006, *Numerical Optimization*, Springer Series in Operations Research and Financial Engineering.
[52] Wegstein, J. H., 1958, "Accelerating Convergence of Iterative Processes," Commun. ACM, **1**(6), pp. 9–13.